Supporting Information for

Kinetic Effects in the Photomediated Synthesis of Silver Nanodecahedra and Nanoprisms: Combined Effect of Wavelength and Temperature

*Haitao Wang[1], Xiaoqiang Cui[1] *, Weiming Guan[2], Xianliang Zheng[1], Hetong Zhao[1], Zhao Wang[1], Qiyu Wang[1], Tianyu Xue[1], Chang Liu[1], David J. Singh[1,3] and Weitao Zheng [1] **

[1] Department of Materials Science, School of Materials Science & Engineering, Key Laboratory of Automobile Materials of MOE and State Key Laboratory of Superhard Materials, Jilin University, Changchun 130012, People's Republic of China

[2] State Key Laboratory of Advanced Technologies for Comprehensive Utilization of Platinum Metals, Kunming, 650106, People's Republic of China

[3]Materials Science and Technology Division, Oak Ridge National Laboratory, Oak Ridge, TN 37831-6056, USA

*E-mail: xqcui@jlu.edu.cn (X. C.) or wtzheng@jlu.edu.cn (W. Z.)

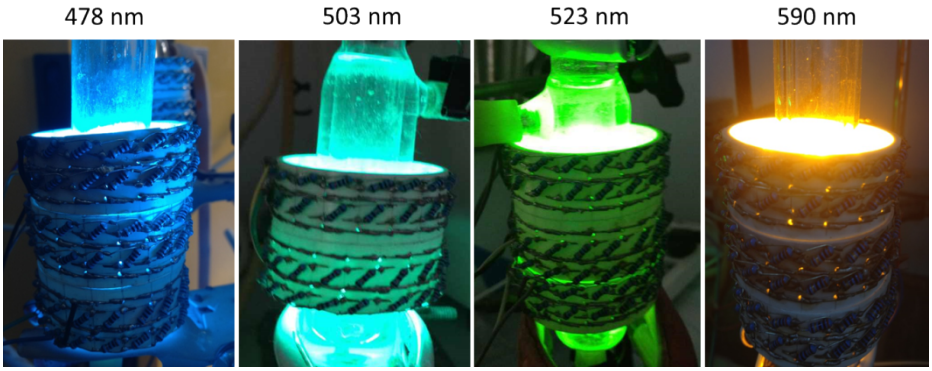

Fig. S1. Photo images of homemade cylindrical LEDs arrays with various wavelengths (478, 503, 523, and 590 nm).

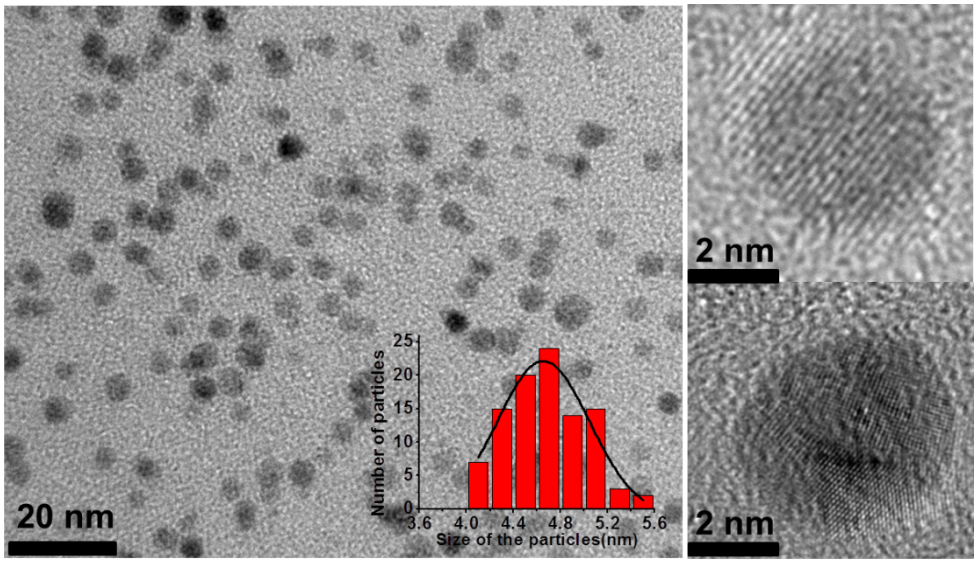

Fig. S2. Left: TEM image of silver seeds in ice bath without photomediated treatment. The inset shows the size distribution of silver seeds. Right: Both single-crystal and multitwinning seeds are observed.

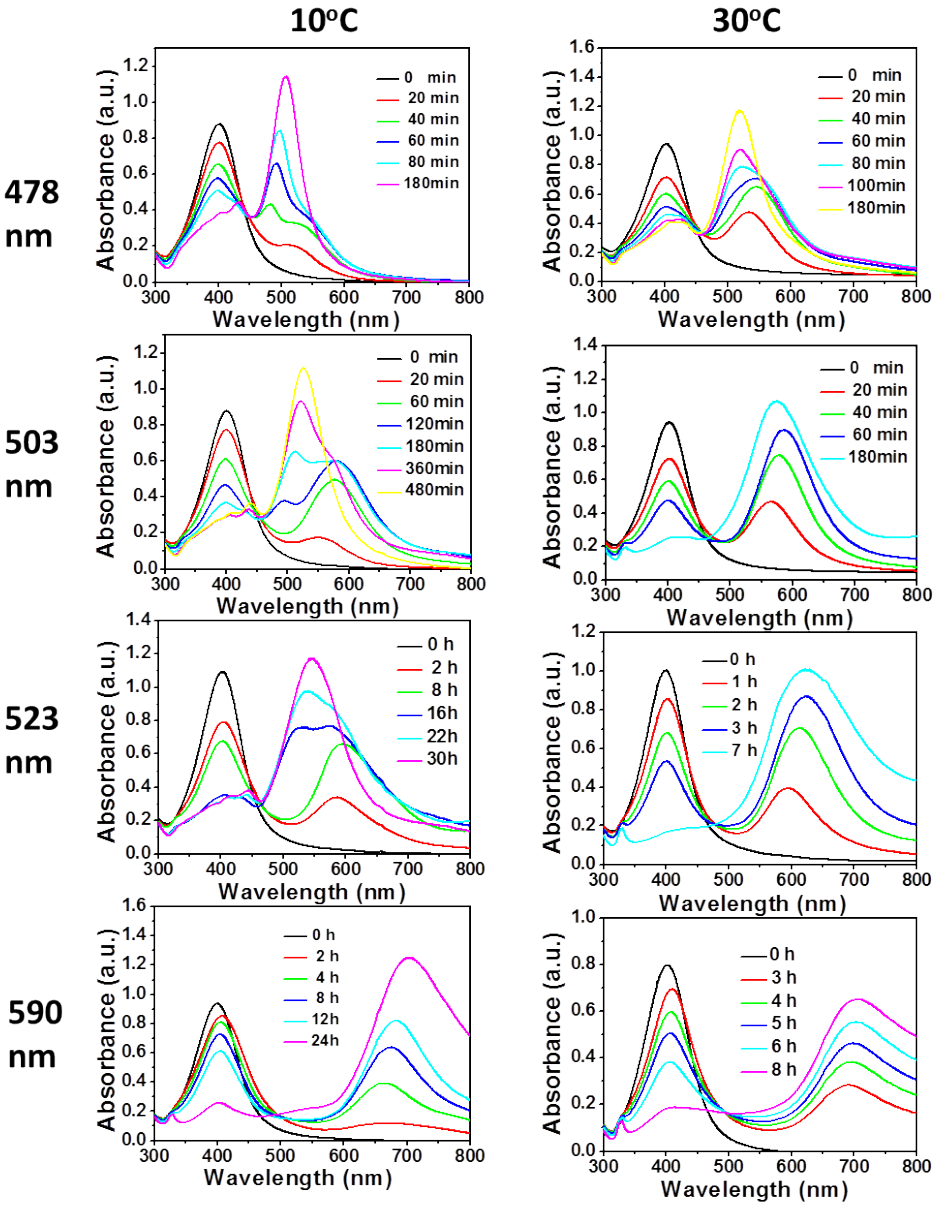

Fig. S3. Time evolution of UV-vis absorbance spectra of silver colloids synthesized at various irradiation wavelengths (478, 503, 523, and 590 nm) and reaction temperatures (10 and 30 °C).

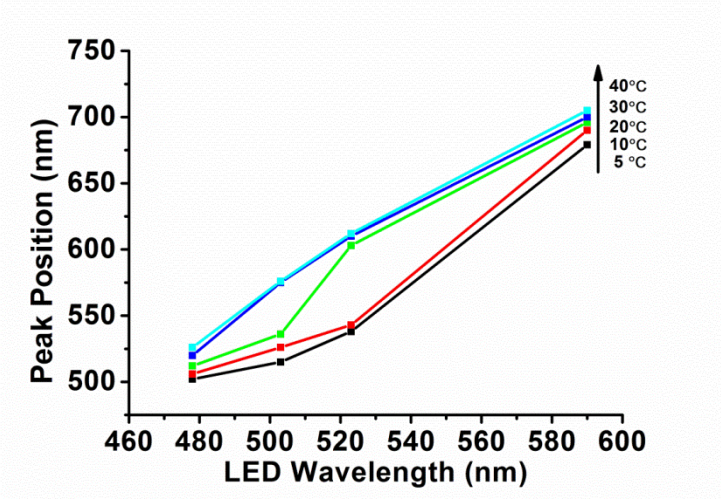

Fig. S4. Plots of the LSPR peak positions from different silver nanoparticles as a function of LED wavelengths.

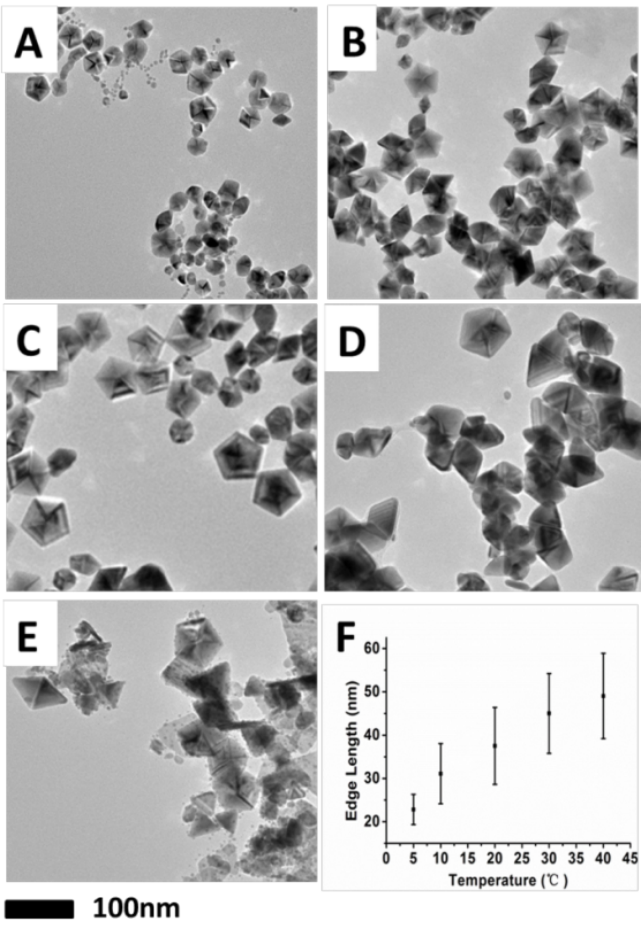

Fig. S5. TEM images of the final products synthesized with 478 nm LED irradiation at different reaction temperatures of： (A) 5 °C，(B) 10 °C，(C) 20 °C，(D) 30 °C, (E) 40 °C (Scale bars: 100nm). (F) Plots of the edge lengths of the silver nanodecahedra as a function of temperature.

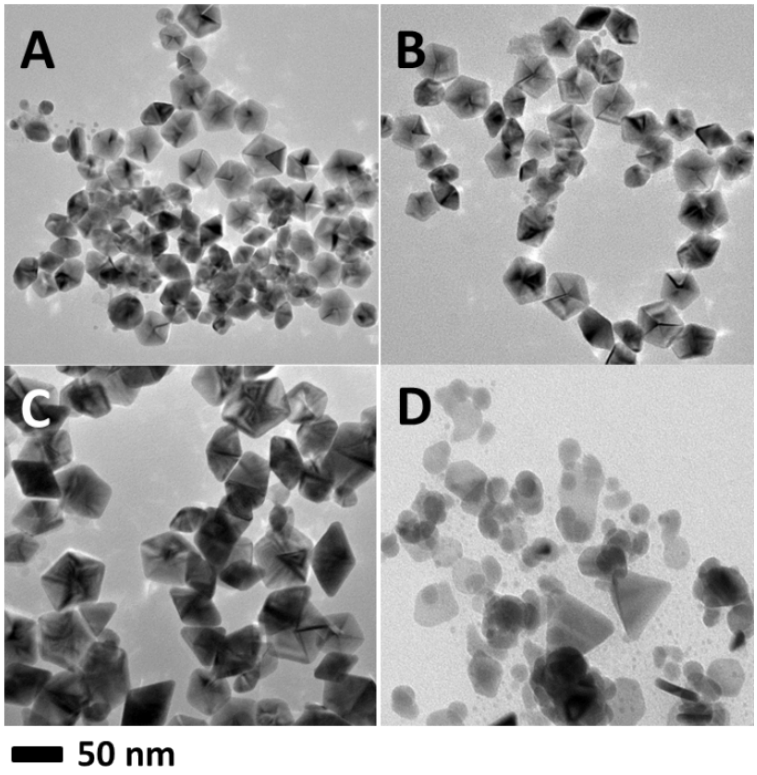

Fig. S6. TEM images of the final products synthesized at **5 °C** with LED irradiation wavelengths of: (A) 478 nm; (B) 503 nm; (C) 523 nm; (D) 590 nm.

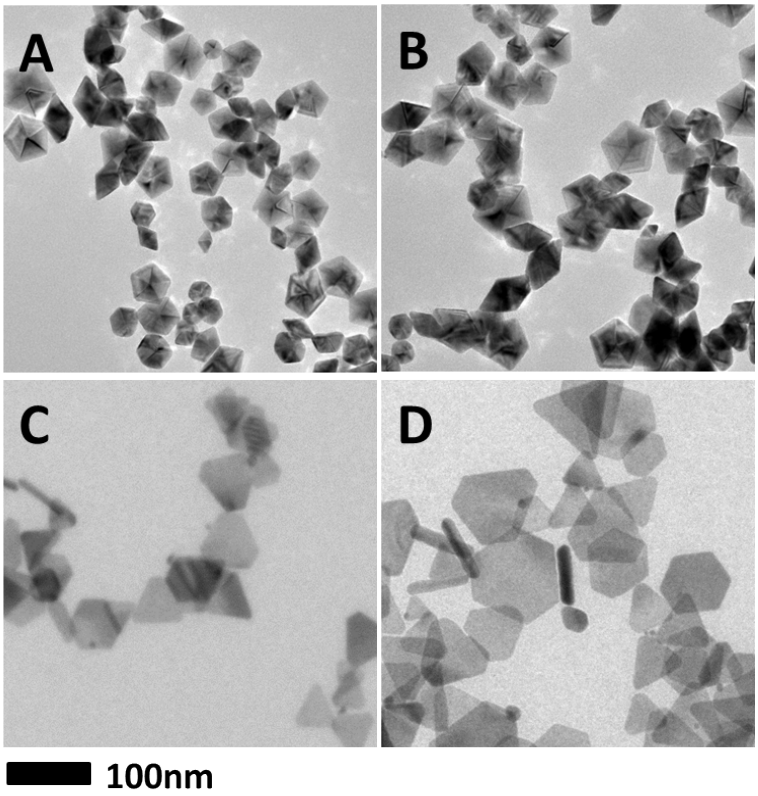

Fig. S7. TEM images of the final products synthesized at **20 °C** with LED irradiation wavelengths of: (A) 478 nm; (B) 503 nm; (C) 523 nm; (D) 590 nm.

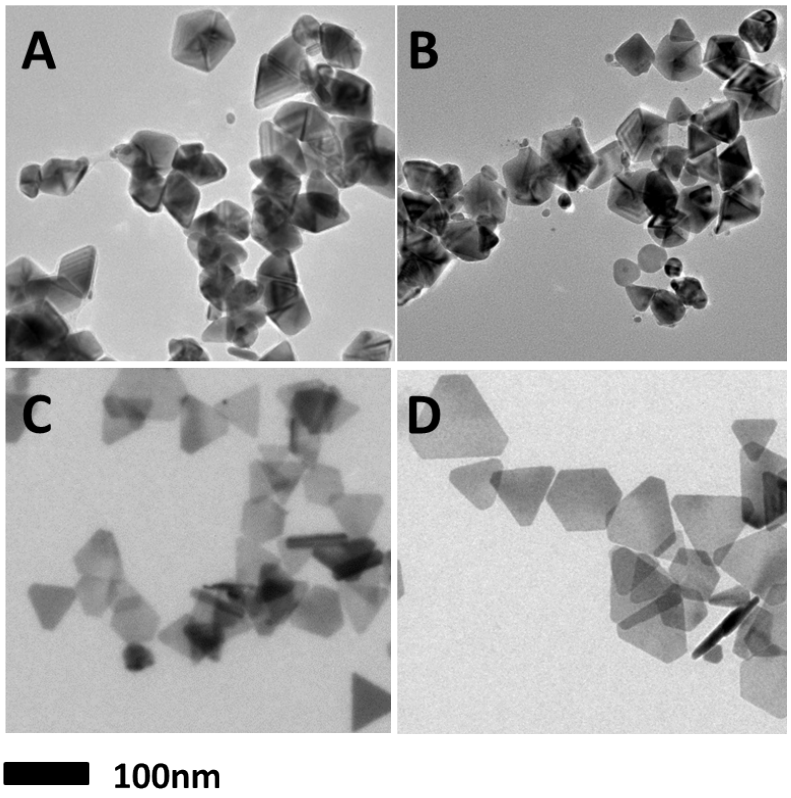

Fig. S8. TEM images of the final products synthesized at **30 °C** wih LED irradiation wavelengths of: (A) 478 nm; (B) 503 nm; (C) 523 nm; (D) 590 nm.

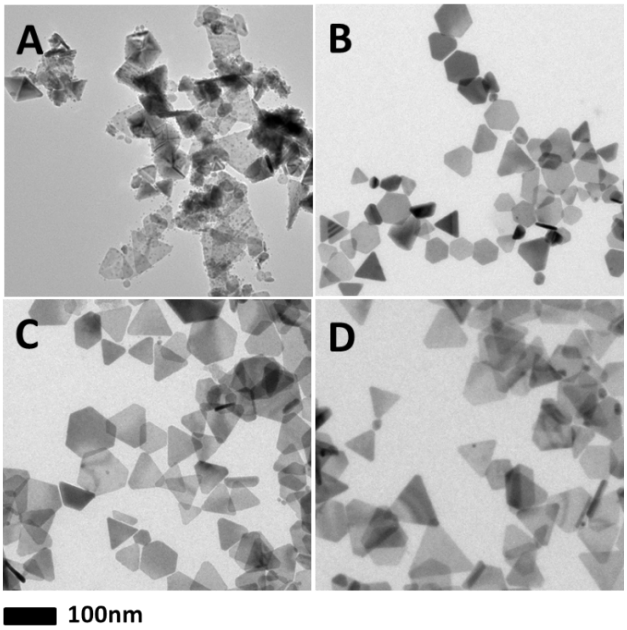

Fig. S9. TEM images of the final products synthesized at **40 °C** with LED irradiation wavelengths of: (A) 478 nm; (B) 503 nm; (C) 523 nm; (D) 590 nm.

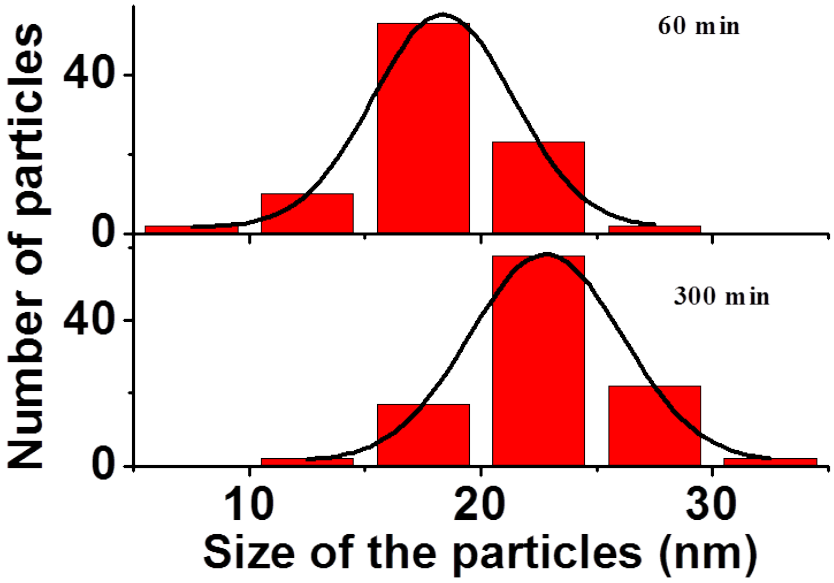

Fig. S10. Histograms of the edge lengths of silver nanodecahedra prepared by 478 nm LED irradiation at 5 °C for 60 min and 300 min, respectively.

Kinetics at 478 nm LED irradiation

The rates of seeds consumption and nanoprisms (or nanodecahedra) formation increase with increasing temperature. The rates of seeds consumption and nanodecahedra formation are slow at a lower temperature of 5 °C, and no nanoprisms are formed. When the reaction temperature is raised, the reaction rate is increased. The nanoprisms are formed at **Stage** Ⅰ and then transformed into nanodecahedra at **Stage** Ⅱ, at three different reaction temperatures of 10, 20 , and 30 °C. Significant distinction can be observed at 40 °C: the absorbance percentage of nanoprisms keep continuously increasing; while only a fraction of nanodecahedra are formed, which is different from that of 503 nm LED irradiation.

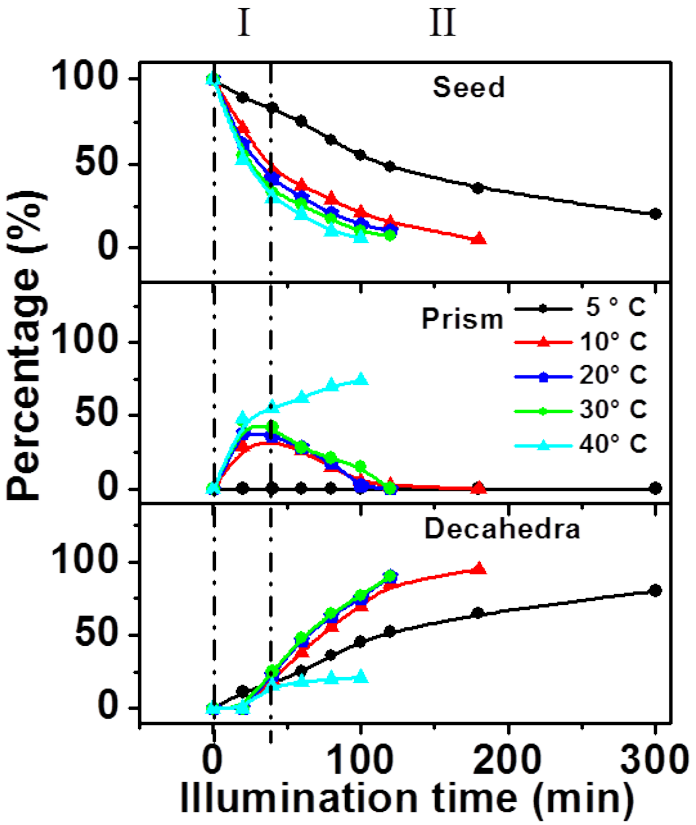

Fig. S11. Corresponding absorbance percentage of seeds, prisms, and decahedra during 478 nm LED irradiation at different reaction temperatures as a function of

illumination time.

Kinetics at 523 nm LED irradiation

Corresponding absorbance percentage of seeds, prisms, and decahedra during 523 nm LED irradiation at different reaction temperatures as a function of illumination time are shown in Fig. S11. The reaction rates are much slower at 5 and 10 °C. The analogous curves indicate the formation of nanoprisms at **Stage I**, and then transformation to nanodecahedra at **Stage Ⅱ**. The reaction at 20, 30, and 40 °C displays similar kinetics. In general, as the reaction temperature increases, the rate of silver nanoprisms formation increases.

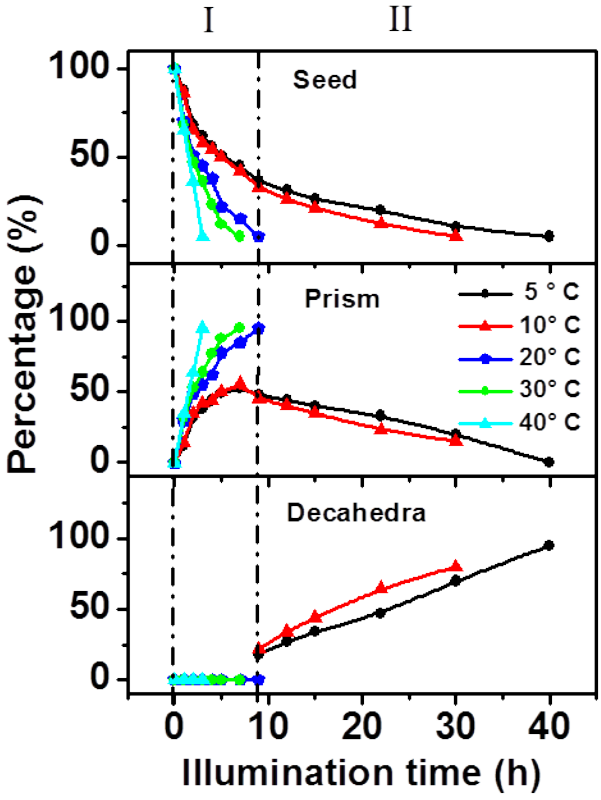

Fig. S12. Corresponding absorbance percentage of seeds, prisms, and decahedra during 523 nm LED irradiation at different reaction temperatures as a function of illumination time.

Kinetics at 590 nm LED irradiation

Silver nanoprisms are sole products at five different reaction temperatures (5, 10, 20, 30 and 40 °C) with 590 nm LED irradiation. The rates of silver seed consumption and formation of nanoprisms rise as the temperature increases (Fig. S13). Two distinctive stages can be identified in nanoprisms formation: At **Stage Ⅰ**, the rate of nanoprisms formation is fast, and when the silver seed are consumed, the reaction rate slow down (**Stage Ⅱ**).

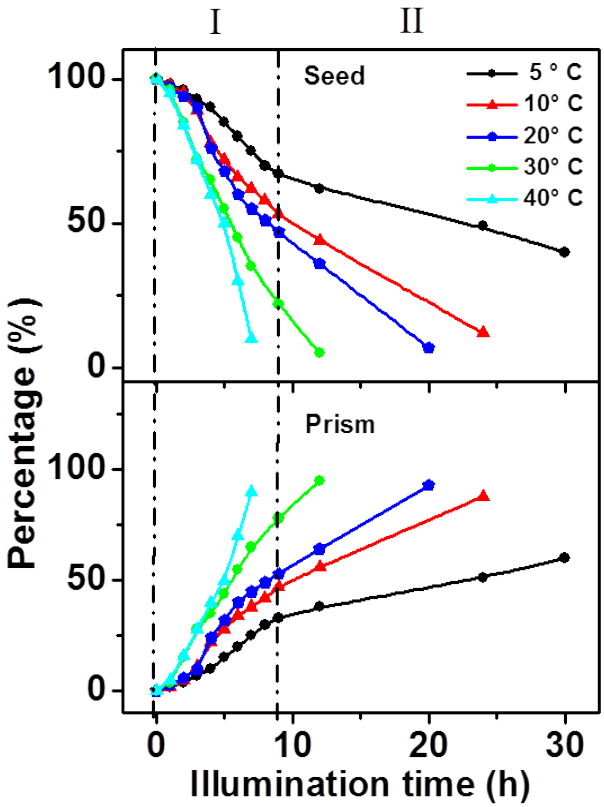

Fig. S13. Corresponding absorbance percentage of seeds, prisms, and decahedra during 590 nm LED irradiation at different reaction temperatures as a function of illumination time.

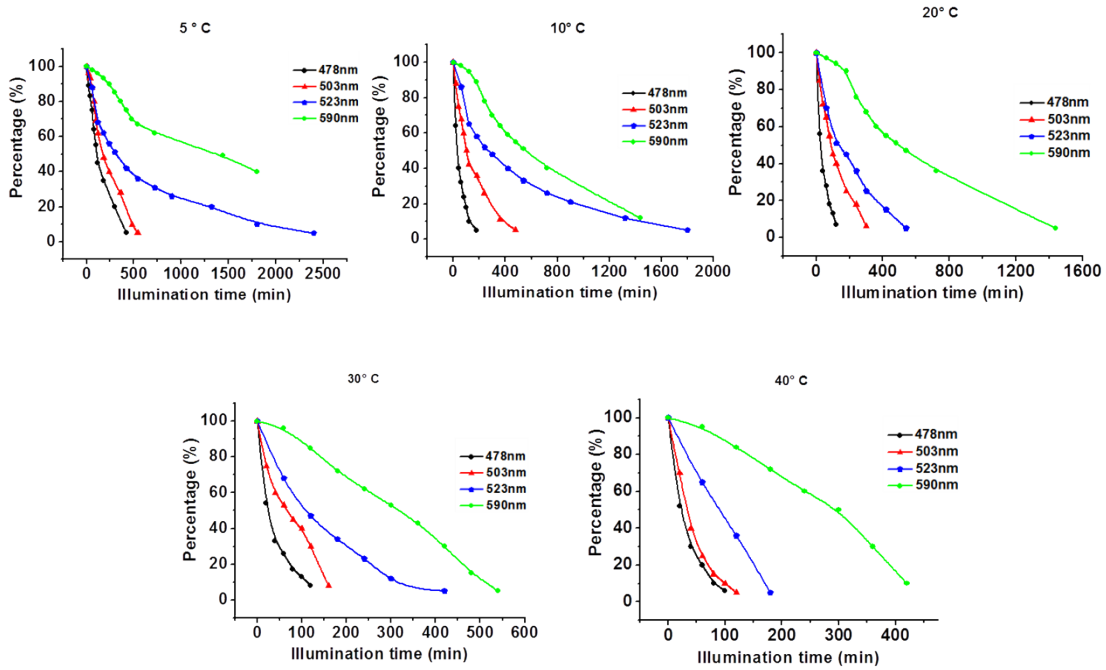

Fig. S14. Corresponding absorbance of seeds during different wavelength irradiation at different reaction temperatures as a function of illumination time.

Primary Process and Secondary Process

It can be noticed that the reaction rate is relatively slow at induction time, which has also been observed by previous reports.[1-2] We propose the induction time in the photomediated reaction can be ascribed to the primary process of photomediated reaction (equation 1). The silver nanoparticles absorbs the photon and then transits to the excited states (Ag*) under LED irradiation. The reduction of Ag^+ by citrate and $NaBH_4$ can be initiated under irradiation at various wavelengths. Citrate is degraded into acetonedicarboxylate. The major role of oxygen is to chemically convert the silver nanoparticles into Ag^+, which is subsequently used as the Ag^+ source for the photoreaction to form prisms or decahedra.[3] Different wavelengths lead to different excited-state energies.[4] Silver nanoparticles under a shorter wavelength irradiation can

efficiently overcome the energy barrier in the primary process, and result in the formation of both nanoprisms and nanodecahedra. Nanodecahedra are formed at a slow reaction rate, and a faster reaction rate leads to the formation of nanoprisms. This can be attributed to secondary process (equation 2, 3), in which a series of kinetic processes occur. However, lower energy (LE) resulting from longer irradiation wavelength, leads to sole product of nanoprisms. Since the dipole plasmon excitation induces an ultrafast charge separation on the nanoparticle surface, this likely leads to the face-selective Ag^+ ions reduction, thereby causing an anisotropic crystal growth. Alternatively, Ag^+ ions selectively adsorbed on different faces, which leads to the subsequent selective deposition of Ag on various faces, resulting in the formation of nanoprisms or nanodecahedra through a thermal process. Growth on {110} facets results in the formation of nanoprisms, while, deposition on {111} results in the formation of nanodecahedra.

Primary process: $Ag^+ + AgNP + Citrate \xrightarrow{hv} Ag^*\text{-}Citrate$ (1)

Secondary process: $Ag^+ + Ag^*\ (LE)\text{ -Citrate} \longrightarrow Ag^0 + acetonedicarboxylate \xrightarrow{\{110\}} Ag_{prism}$ (2)

$Ag^+ + Ag^*\ (HE)\text{ -Citrate} \longrightarrow Ag^0 + acetonedicarboxylate \xrightarrow{\{111\}} Ag_{dec}$ (3)

Arrhenius Plots

The plots of *ln c* vs. time were obtained from the data in Fig. 7, S11-S13. Fig. S15 shows that linear relationship of seeds consumption with respect to time. The value of *c* was defined as intensity of seeds. These observations indicate that the consumption of seeds follows the first order dependence with respect to the reaction time.

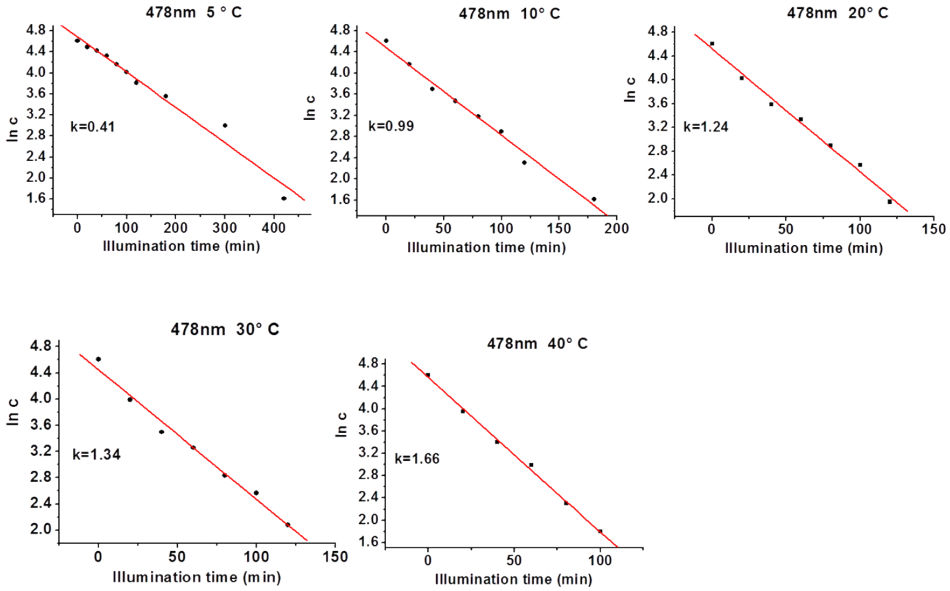

Fig. S15. Plots of *ln c* vs. time were obtained by 478 nm LED irradiation at various reaction temperatures.

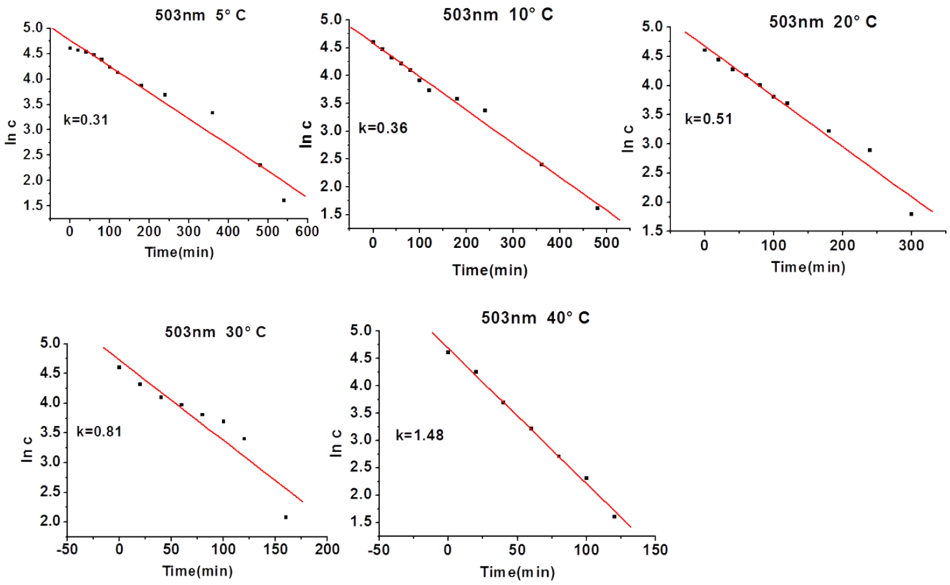

Fig. S16. Plots of *ln c* vs. time were obtained by 503 nm LED irradiation at various reaction temperatures.

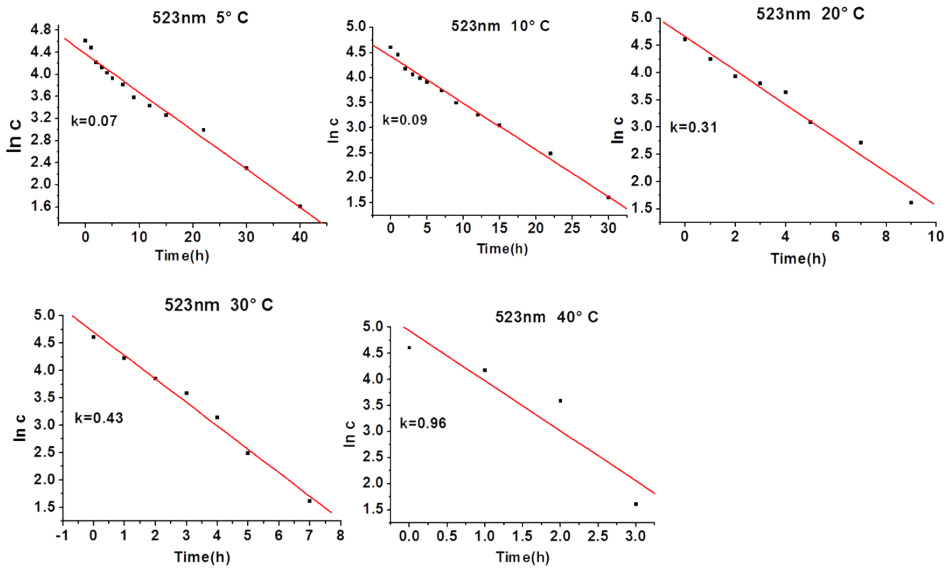

Fig. S17. Plots of *ln c* vs. time were obtained by 523 nm LED irradiation at various reaction temperatures.

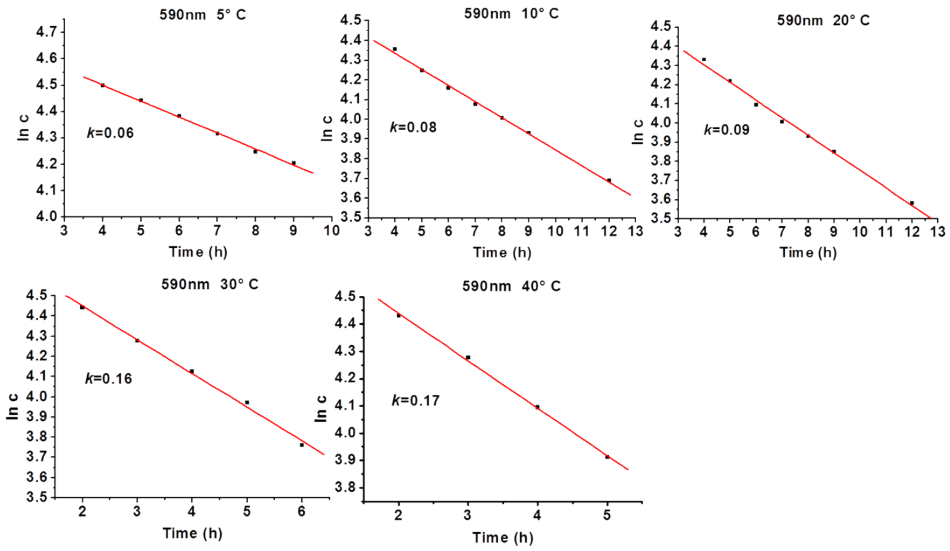

Fig. S18. Plots of *ln c* vs. time were obtained by 590 nm LED irradiation at various reaction temperatures.

The value of rate constant (*k*) was the slope of fitting lines. Arrhenius plots obtained at various irradiation wavelengths, *lnk vs 1/T*.

Table S1. Parameters of the Arrhenius equation $k = A\ exp\ (-E_a/RT)$ under various LED irradiation.

Wavelength (nm)	*ln*(A /h^{-1})	E_a/kJ mol^{-1}
478	10.6±1.83	25.9±4.5
503	12.6±1.2	31.4±2.9
523	20.5±1.9	53.7±4.8
590	6.8±1.45	22.2±3.5

Five-fold Twinning Particles Are Involved from Planar Structure

To verify the five-fold twinning particles are involved from the planar structure, we etch silver nanoprisms (0.1 mM Ag, 10 mL) by adding chloride ions (1M, 10 μL) (Fig. S19A), and the products were irradiated with 478 nm LEDs at 20 °C. Majority of the products transformed to silver nanodecahedra (Fig. S19B). And then silver nanodecahedra (0.1 mM Ag, 10 mL) were etched by adding hydrochloric acid (1M, 10 μL) (Fig. S19C), and the products were irradiated with 523 nm LEDs at 40 °C. The bigger silver nanodecahedra can be observed, but no nanoprisms formed (Fig. S19D). This observation suggested that the planar structure silver nanoparticles can transformed to five-fold twinning particles, but it is irreversible.

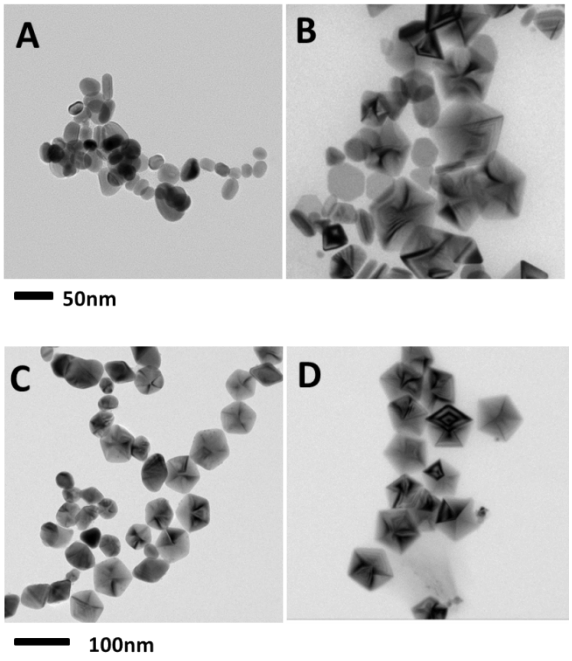

Fig. S19. TEM images showing of (A) the etched silver nanoprisms (B) products obtained further with 478 nm LEDs irradiation at 20 °C; TEM images showing of (C) the etched silver nanodecahedra and (D) products obtained further with 523 nm LEDs irradiation at 40 °C.

Reversibility Research

Silver nanodecahedra were synthesized with 478 nm LEDs irradiation of seeds at 5 °C. The nanodecahedra solution was then irradiated with 478 nm at 40 °C. Silver nanoprisms synthesized with 523 nm LEDs irradiation of seeds at 40 °C. Silver nanoprisms solution was then irradiated with 478 nm at 5 °C. The unchanged spectra suggest the when the silver nanodecahdra or nanoprisms formed, it is not reversible when the reaction condition changed (Fig. S20).

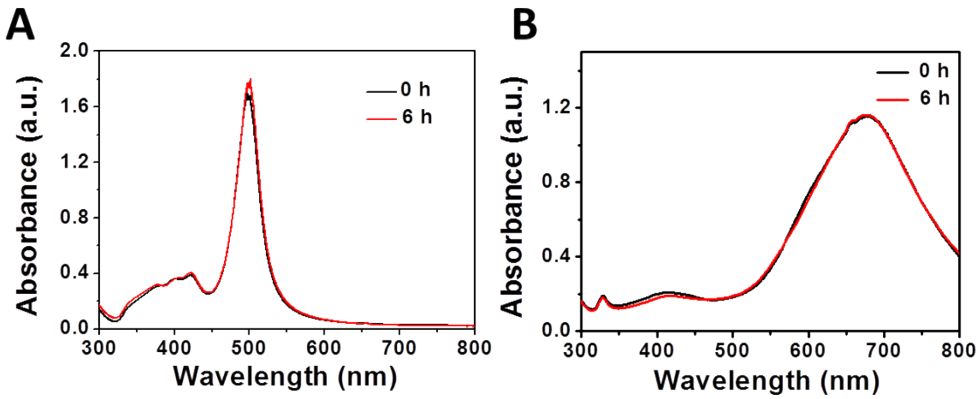

Fig. S20. (A) UV-vis spectra of irradiation of silver nanodecahedra with 523 nm at 40 °C. (B) UV-vis spectra of irradiation of silver nanoprisms with 478 nm at 5 °C.

Temperature Effects on Platelet and Five-Fold Twinning Structure Seeds

The temperature of pre-storage conditions did not affect the final products of the photomediated synthesis. If seeds were bubbled with N_2 and allowed to age overnight at 40 °C in the dark, then irradiation with 478 nm LEDs at 5 °C, products were nanodecahedra; while when seeds were bubbled with N_2 and allowed to age overnight at 5 °C in the dark, then irradiation with 478 nm LEDs at 40 °C, the silver colloid exhibited two major absorbance bands, indicating the formation of a bimodal size distribution nanoprisms (Fig. S21). This observation is consistent with the previous reports.[5] These results indicate the platelet structure and five-fold twinning structure seeds are formed during the photomediated synthesis independent of pre-storage conditions.

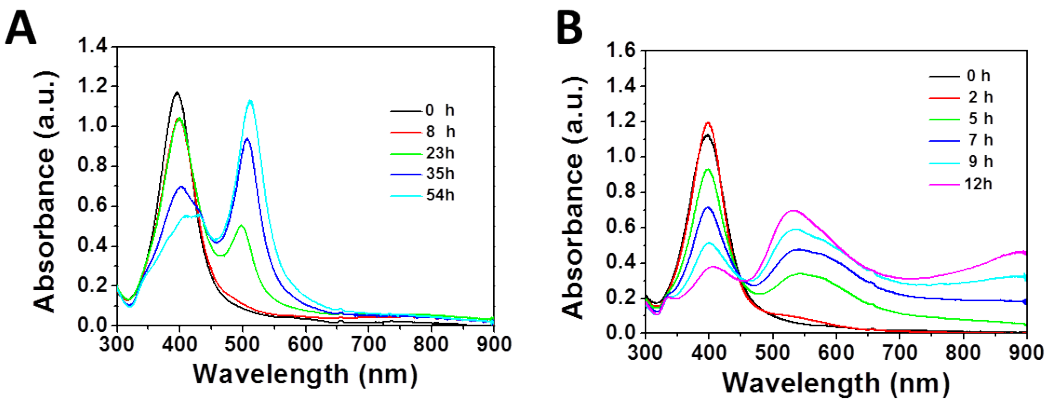

Fig. S21. UV-vis spetra of silver seed bubbled with N_2 (A) aged overnight at 40 °C in the dark, then irradiation with 478 nm LEDs at 5 °C; (B) aged overnight at 5 °C in the dark, then irradiation with 478 nm LEDs at 40 °C.

Transformation of the Mixture of Seeds and Nanodecahedra or Nanoprisms under Kinetically and Thermodynamically Favored Conditions:

To further investigate the shape transformation phenomenon, we mixed silver nanodecahedra (50 nm) with seeds and then irradiating with 523 nm LEDs at 40 °C, which is a kinetic controlled condition. Although the LSPR peaks of nanoprisms were observed at first, the final products are solely bigger nanodecahedra, no nanoprisms are formed. That means that when the sizes of nanodecahedra are big enough, the reaction will still go to thermodynamic controlled. Oswald ripenning rules the vanishing of the seeds and redepostion on the as-prepared nanodecahedra (Fig. S22).

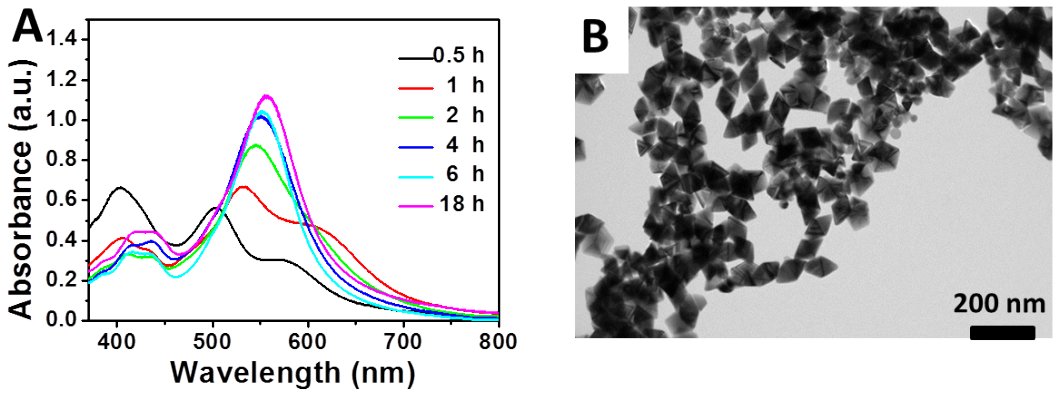

Fig. S22. (A) Time evolution of UV-vis spectra with 523 nm LEDs irradiation of mixture of silver nanodecahedra (5 mL) and seed (5 mL) at 40 °C. (B) TEM image of the final product after 18 h irradiation.

Silver nanoprisms (5 mL, 60 nm) were mixed with as-prepared seeds (5 mL) and then the mixture was irradiated with 478 nm LEDs at 10 °C, which is a thermodynamic controlled condition. Nanodecahedra were also formed with the slightly vanishment of LSPR from nanoprisms. Nanoprisms were dissolved and became truncated as indicated in Fig. S23 B. These results were also consistent with

the mechanisms described in Fig. 9, the nanodecahedra are more stable than nanoprism, owing to the lower energy of nanodecahedra.

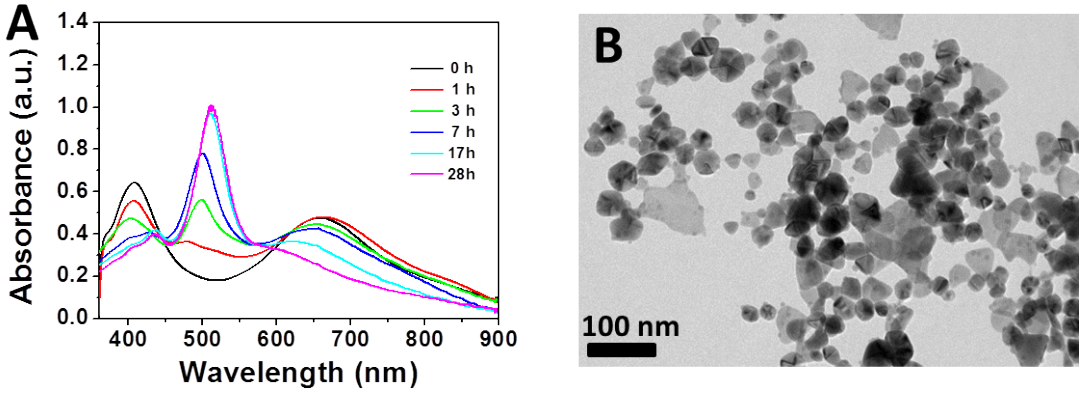

Fig. S23. (A) Time evolution of UV-vis spectra with 478 nm LEDs irradiation of the mix solution of nanoprisms and as-prepared seeds at 10 °C. (B) TEM image of the final product after 28 h irradiation.

Effect of Intensity

We also investigated the effect of changing the light intensity since the reaction rate in kinetics process can be influenced by the intensity. The as-prepared seeds were irradiated with a wavelength of 478 nm at 40 °C using a filter with various transmittances of 15%, 25%, 70%, and 100%, respectively. The reaction rate increased with increasing of the intensity. The products obtained at various intensities were mixture of silver nanoprisms and nanodecahedra. The reaction rate at 40 °C with transmittances of 15% decreases to a value similar to that obtained at 5 °C with transmittances of 100% (Fig. S24, 25). The products were mixture of silver nanoprisms and nanodecahedra (Fig. S26). When the intensity was decreased, the formation rates of both nanoprisms and nanodecahedra decreased. The transformation process that controls the final morphology and involves a competition between the kinetics and the thermodynamics is governed by reaction temperature. Silver

nanodecahedra were the final products favored by thermodynamic control at lower temperatures.

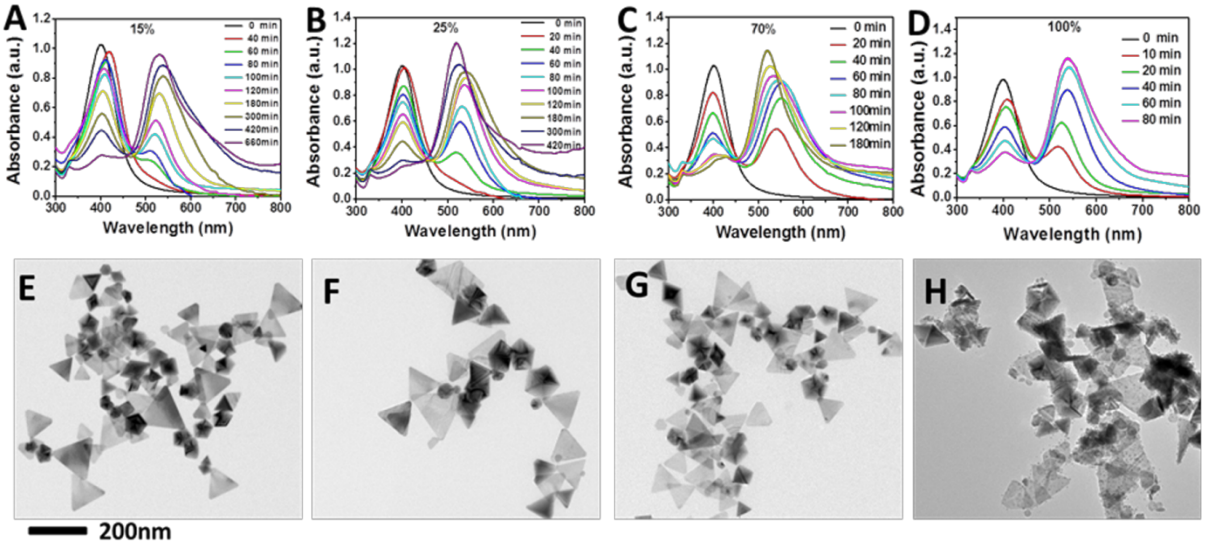

Fig. S24. Time evolution of UV-vis spectra with 478 nm LEDs irradiation of as-prepared seeds with various transmittances at 40 °C: (A) 15%; (B) 25%; (C) 70%; (D) 100%. TEM image of the final product with various transmittances: (E) 15%; (F) 25%; (G) 70%; (H) 100%.

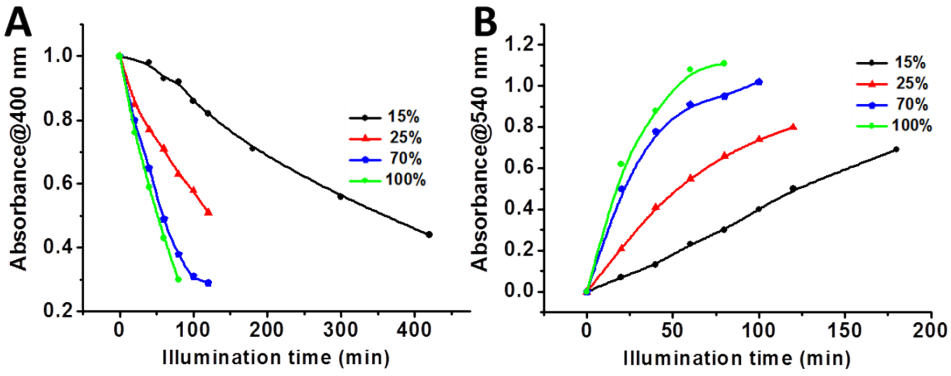

Fig. S25. Absorbance at (A) 400 nm and (B) 540 nm of the colloid solutions synthesized with 478 nm LEDs irradiation at 40 °C at different transmittance vs illumination time.

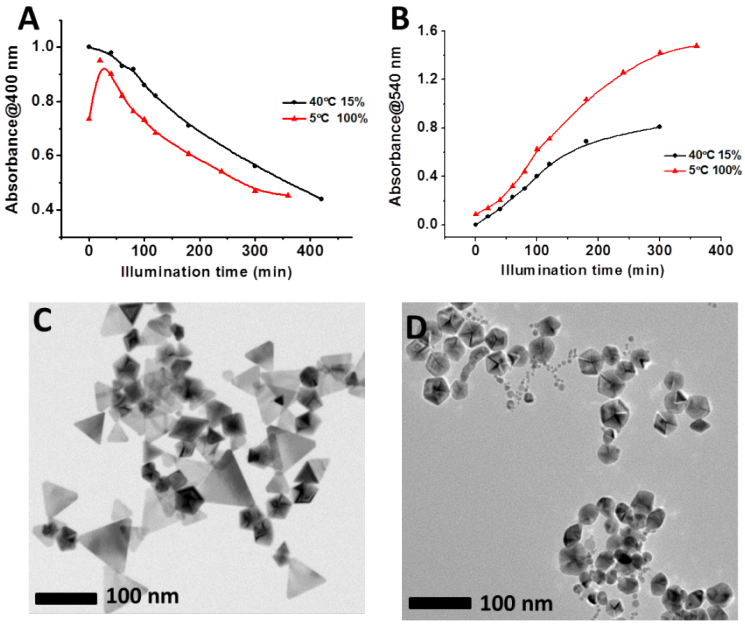

Fig. S26. Absorbance at (A) 400 nm and (B) 540 nm of the colloid solutions synthesized at different reaction condition vs illumination time. TEM image of the final product irradiated with transmittance of (C) 15% at 40 °C, (D) 100% at 5 °C.

Effect of Concentrations

It should be pointed out that kinetics could also be influenced by the concentration. So we conducted the experiment to investigate the role of concentrations of reactants played in the kinetic process. 0.1mL $AgNO_3$ (10 mM) was added to the as-prepared seed, and the resulting silver solution was then irradiated with 503 nm LEDs irradiation at 10 °C (Fig. S27 C, D). The other comparative silver seed was irradiated under the same conditions without extra $AgNO_3$ (Fig. S27 A, B). As expected, the reaction rate is faster after increasing the concentration, similar to the condition of increasing temperature. The formation rate of nanoprisms is faster after increasing the concentration, but final product is still nanodecahedra. It can be concluded both increasing the reaction temperature and the concentration of reactants

can improve the reaction rates. Silver nanodecahedra were the final products favored by thermodynamic control.

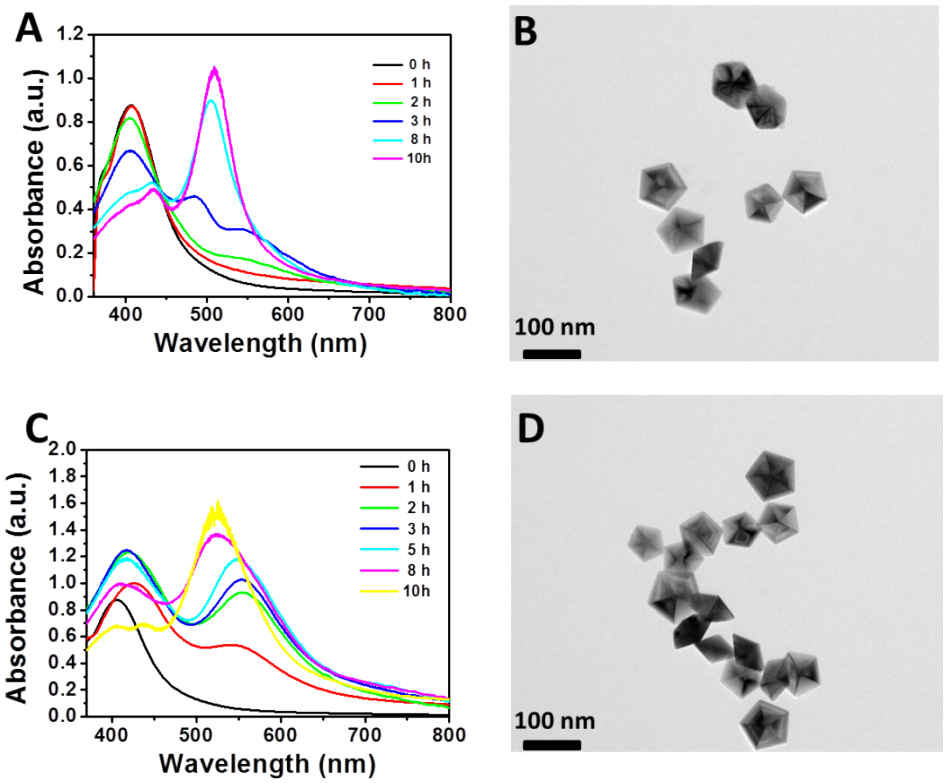

Fig. S27. (A) Time evolution of UV-vis spectra of silver nanodecahedra synthesized with 503 nm LEDs irradiation of seed at 10 °C; (B) TEM image of the final product after 10 h irradiation; (C) Time evolution of UV-vis spectra of 10 mL silver seed and then mixing with 0.1mL $AgNO_3$ (10 mM) irradiation with 503 nm LEDs irradiation at 10 °C ; (D) TEM image of the final product after 10 h irradiation.

References

1 Rongchao Jin, Y. C., Chad A. Mirkin, K. L. Kelly,George C. Schatz, J. G. Zheng, *Science* **2001,** *294*, 1901-1903.

2 George P. Lee, Y. S., Ellen Lavoie, Torben Daeneke, Philipp Reineck, Ute B. Cappel, David M. Huang and Udo Bach, *ACS Nano* **2013,** *7*, 5911-5921.

3 Xue, C.; Metraux, G. S.; Millstone, J. E.; Mirkin, C. A., *J. Am. Chem. Soc.* **2008,** *130*, 8337-8344.

4 Zhang, J. A.; Langille, M. R.; Mirkin, C. A., *J. Am. Chem. Soc.* **2010,** *132*, 12502-12510.

5 Rongchao Jin, Y. C. C., Encai Hao, Gabriella S. Me´ traux,; Mirkin, G. C. S. C. A., *Nature* **2003,** *425*, 487-490.